Evidence for Nonlocal Electrodynamics in Planar Josephson Junctions

A. A. Boris,[1] A. Rydh,[1] T. Golod,[1] H. Motzkau,[1] A. M. Klushin,[2] and V. M. Krasnov[1]

[1]*Department of Physics, AlbaNova University Center, Stockholm University, SE-106 91 Stockholm, Sweden*
[2]*Institute of Physics of Microstructures, 603950 Nizhnij Novgorod, Russia*

We study the temperature dependence of the critical current modulation $I_c(H)$ for two types of planar Josephson junctions: a low-T_c Nb/CuNi/Nb and a high-T_c YBa$_2$Cu$_3$O$_{7-\delta}$ bicrystal grain-boundary junction. At low T both junctions exhibit a conventional behavior, described by the local sine-Gordon equation. However, at elevated T the behavior becomes qualitatively different: the $I_c(H)$ modulation field ΔH becomes almost T independent and neither ΔH nor the critical field for the penetration of Josephson vortices vanish at T_c. Such an unusual behavior is in good agreement with theoretical predictions for junctions with nonlocal electrodynamics. We extract absolute values of the London penetration depth λ from our data and show that a crossover from local to nonlocal electrodynamics occurs with increasing T when $\lambda(T)$ becomes larger than the electrode thickness.

Josephson junctions are usually formed by a barrier sandwiched between two superconducting electrodes, as sketched in Fig. 1(a). Such overlap-type junctions have a local electrodynamics, described by a differential sine-Gordon equation [1]. The locality is caused by the smallness of the London penetration depth λ, at which the magnetic field is screened in the electrodes, in comparison with the Josephson penetration depth λ_J, at which the field is varied along the junction $\lambda_J \gg \lambda$. In this case the field is locked inside the junction. Its distribution is quasi-one-dimensional and depends only on local, instantaneous values of the Josephson phase difference. However, if the effective penetration depth becomes larger than λ_J, the magnetic field is no longer locked in the junction. The field distribution becomes two-dimensional and is determined by a nonlocal integrodifferential equation involving phases in the whole junction [2].

It has been suggested that nonlocal electrodynamics can be realized in planar junctions formed at the edge between two superconducting films with the thickness $d < \lambda$ [2–7]. Incomplete screening by thin films leads to an increase of the effective penetration depth. For $d \ll \lambda$ it is equal to the Pearl length $\Lambda = 2\lambda^2/d \gg \lambda$. Furthermore, unlike in the case of overlap junctions, the field should be applied perpendicular to the films. This leads to the appearance of a large demagnetization factor (flux focusing) [3,4,8] and causes the spreading of stray magnetic fields at the surface of superconducting electrodes to a distance of the order of the junction width $w \gg \lambda$, as sketched in Fig. 1(b). In recent years several types of planar junctions have been studied, including high-T_c grain-boundary junctions [9–12] and proximity-coupled junctions via semiconducting heterostructures [13,14], ferromagnets [14–16], normal metals [17,18], or graphene [19]. The effect of flux focusing has been established in previous works [3,8,9], but the role of nonlocality remains to be clarified.

Theoretically it has been predicted that properties of nonlocal and local junctions should be significantly different [4–7]. The difference is summarized in Table I. For example, in local junctions the Josephson critical current I_c as a function of applied magnetic field H exhibits periodic-in-field Fraunhofer modulation with a period $\Delta H \simeq \Phi_0/2w\lambda$, where Φ_0 is the flux quantum. The T dependence of ΔH is determined by $\lambda(T)$. Close to T_c, $\lambda(T)$ diverges and ΔH vanishes as $(T_c - T)^{1/2}$. On the other hand, for nonlocal junctions the $I_c(H)$ is not perfectly periodic in the field and ΔH is determined by the spreading of stray fields, which depends solely on the geometry w and should be T independent. Therefore, an analysis of the T dependence of $I_c(H)$ close to T_c should provide a clear distinction between the local and nonlocal models.

In this work we experimentally study T dependencies of the $I_c(H)$ modulation for two types of planar thin-film junctions: a low-T_c Nb/CuNi/Nb and a high-T_c YBa$_2$Cu$_3$O$_{7-\delta}$ (YBCO) bicrystal grain-boundary junction. We observe that at low T, junctions can be described by local electrodynamics. However, at elevated T both junctions exhibit a qualitatively different behavior, consistent with the occurrence of the nonlocal electrodynamics. We show that a temperature-driven crossover from local to nonlocal electrodynamics, occurs when $\lambda(T)$ becomes larger than the electrode thickness.

Figures 1(c) and 1(d) represent images of a studied junction. The YBCO grain-boundary junction was fabricated on a symmetrical bicrystal yttria-stabilized zirconia substrates ([001] tilt) with a misorientation angle of 24°. To prevent interface reactions, a 40 nm thick CeO buffer layer was deposited prior to depositing the YBCO films. The YBCO film with the thickness $d = 300$ nm and $T_c = 86.5$ K was grown epitaxially by reactive high-oxygen-pressure metal coevaporation using a rotating substrate holder at the Ceraco ceramic coating company [20].
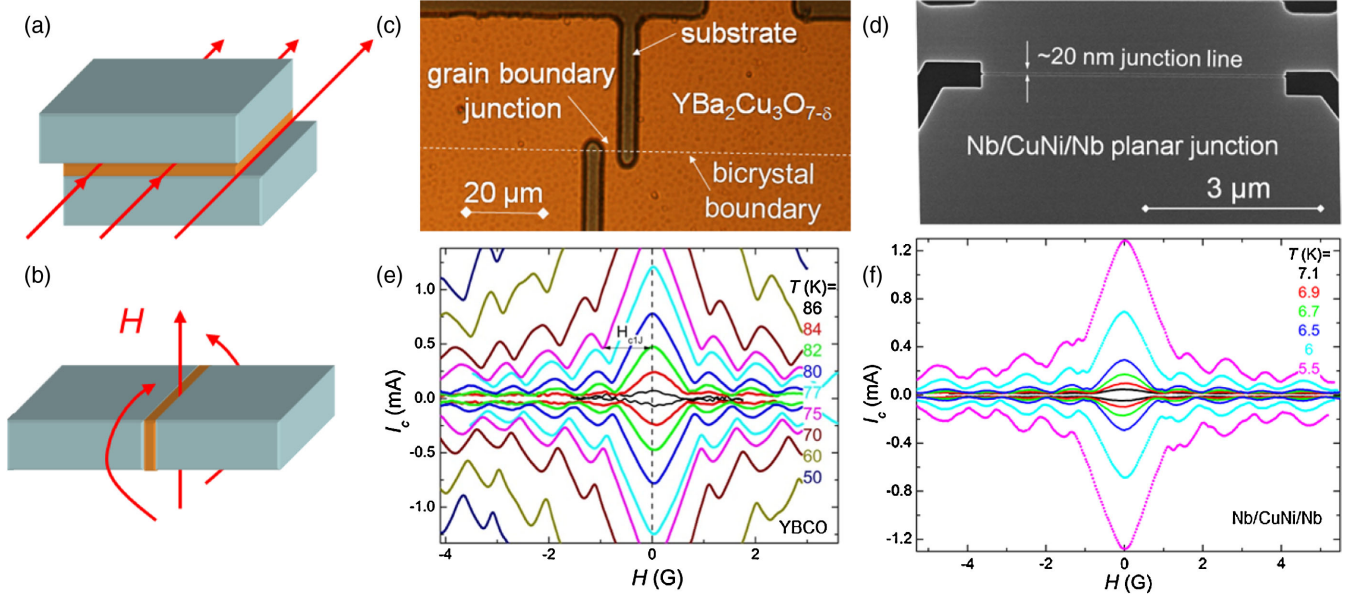
FIG. 1 (color online). Geometries of (a) a conventional overlap-type Josephson junction and (b) a planar Josephson junction in an applied magnetic field H. (c) Top view of the studied YBCO bicrystal junction (optical microscope image). (d) Top view scanning electron microscope image of the studied planar Nb/CuNi/Nb junction. (e), (f) $I_c(H)$ modulation patterns at different temperatures for (e) the YBCO junction and (f) the Nb/CuNi/Nb junction.

The substrate temperature was 665 °C and the deposition rate ~0.4 nm/s. Subsequently, a $w \simeq 6$ μm wide junction was patterned by photolithography and cryogenic Ar^+-ion etching. The details of bicrystal junction fabrication can be found in Refs. [21,22]. A low-T_c Nb/CuNi/Nb planar junction ($T_c = 8.3$ K) was made by the focused ion beam etching of a narrow (~ 20 nm) grove through a Nb/CuNi (70/50 nm) bilayer film. The films were deposited at room temperature on oxidized Si substrates by dc-magnetron sputtering at a base pressure of $\sim 10^{-8}$ Torr and a processing Ar pressure of 5 mTorr. The $Cu_{57}Ni_{43}$ film was deposited by cosputtering from Cu and Ni targets with controlled Ni and Cu deposition rates. The bilayer film was patterned by photolithography and ion etching (CF_4 reactive ion etching for Nb and Ar milling for CuNi). The width of the junction was $w \simeq 5$ μm. The details of the Nb/CuNi/Nb planar junction fabrication can be found in Refs. [14,16]. Measurements were performed in a cryogen-free cryostat using a four-probe configuration. The magnetic field was applied perpendicular to the films, as illustrated in Fig. 1(b).

Figures 1(e) and 1(f) represent measured $I_c(H)$ modulation patterns at different temperatures for the YBCO and the Nb planar junctions, respectively. At low T, the central maxima at $H = 0$ are significantly wider than subsequent lobes in $I_c(H)$ and exhibit a characteristic linear decrease with the field. Such behavior is typical for long junctions, $w > 4\lambda_J$ [1,9,23]. In this case the external magnetic field can be screened within the junction. The linear-in-field central maximum corresponds to the Meissner state without Josephson vortices inside the long junction. It ends at the Josephson lower critical field H_{c1J} [9]. At $H > H_{c1J}$ Josephson vortices penetrate the junction and the $I_c(H)$ modulation is restored. Thus defined, H_{c1J} is marked by the horizontal arrow for the curve at $T = 75$ K in Fig. 1(e). For the Nb junction, Fig. 1(f), the linear-in-field central maximum is seen only at the lowest temperatures.

TABLE I. Characteristic parameters of local overlap-type and nonlocal planar Josephson junctions. Here d_{eff} is the effective magnetic thickness of the junction, i.e., the distance at which the magnetic field decays in the electrodes, $\Delta H = \Phi_0/w d_{eff}$ is the flux-quantization field, corresponding to the field interval of $I_c(H)$ modulation, λ_J is the Josephson penetration depth, $H_{c1J} \simeq 2\Phi_0/\pi^2 \lambda_J d_{eff}$ is the lower critical field for the penetration of Josephson vortices, Φ_0 is the flux quantum, c is the speed of light, d is the thickness of superconducting films, w is the junction width, λ is the London penetration depth, and I_c is the critical current at $H = 0$.

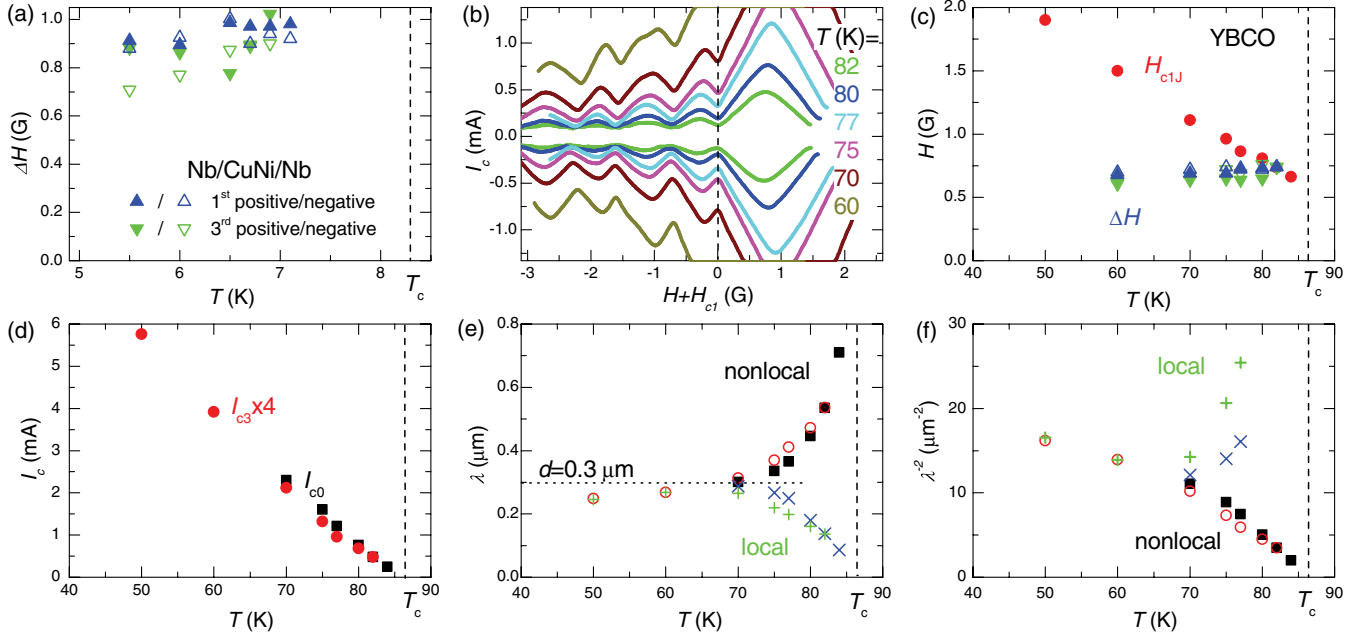| Junction type	Electrodynamics	d_{eff}	ΔH	λ_J	H_{c1J}
Overlap	Local	$\simeq 2\lambda$	$\Phi_0/2w\lambda$	$\sqrt{\Phi_0 cdw/16\pi^2 \lambda I_c}$	$\sqrt{16\Phi_0 I_c/\pi^2 cdw\lambda}$
Planar	Nonlocal	$\sim w$	$1.8\Phi_0/w^2$	$\Phi_0 cdw/16\pi^2 \lambda^2 I_c$	$57.6 I_c \lambda^2/cdw^2$

FIG. 2 (color online).   (a) Measured values of $\Delta H(T)$ for the Nb/CuNi/Nb junction. Blue pointing up triangles represent the width of the first $I_c(H)$ lobe. Green pointing down triangles represent the width of the third lobe. Data are shown for both positive $H > 0$ and negative $H < 0$ fields for $I_c > 0$. (b) Plots of $I_c(H + H_{c1J})$ at different temperatures for the YBCO junction, with the first minimum at $H < 0$ shifted to the origin. Temperature independence of the flux-quantization field ΔH is clearly seen. (c) Measured values of $\Delta H(T)$ (triangles) and $H_{c1J}(T)$ (red circles) for the YBCO junction. Colors of triangles represent the same maxima of Fraunhofer patterns as in (a). (d) Measured dependence $I_{c0}(T)$ for the positive critical current at the central maximum (black squares) and the maximum at the third lobe $I_{c3}(T)$ ($H < 0$, positive current) scaled by a factor 4. (e), (f) Temperature dependencies of λ and λ^{-2} calculated using measured data, equations from Table I, and $H_{c1J}(T)$ and $I_c(T)$ data from panels (c) and (d). Squares and circles show results calculated using equations for nonlocal planar junctions, crosses, and pluses—for local overlap-type junctions.

At elevated T, the $I_c(H)$ starts to resemble a Fraunhofer pattern, characteristic for short junctions, $w \lesssim \lambda_J$ [1]. However, unlike the Fraunhofer modulation, the measured $I_c(H)$ modulation does not have a constant flux-quantization field ΔH. Indeed, from Fig. 1(f) it can be seen that at high T the first minima (half the width of the central maximum) is narrower than the subsequent lobes: $H_1/\Delta H \simeq 0.83$. This is close to the theoretical value 0.8173, calculated by J. R. Clem for short planar junctions [7]. The same ratio $H_1/\Delta H \simeq 0.83$ is observed for the YBCO junction very close to T_c, when the junction becomes short; see the curve at $T = 84$ K in Fig. 1(e).

Triangles in Figs. 2(a) and 2(c) represent the T dependence of ΔH for Nb and YBCO junctions, respectively, obtained from the widths of the first and the third sidelobes of $I_c(H)$ at positive (filled) and negative (open symbols) fields. It is seen that $\Delta H(T)$ is almost constant. It does not show a tendency to vanish at $T \to T_c$, as expected for local junctions, but rather even slightly increases with increasing T. The absolute value $\Delta H \sim 1$ Oe is consistent with the prediction from Table I for nonlocal planar junctions with $w = 5$–6 μm. To clearly see the T independence of ΔH, we replot the $I_c(H + H_{c1J})$ data for the YBCO junction in Fig. 2(b), offset by $H_{c1J}(T)$ so that the first minimum at $H < 0$ is shifted to the origin (dotted vertical line). From

this plot it is clearly seen that the field scale of the $I_c(H)$ modulation is indeed almost T independent.

Circles in Fig. 2(c) represent the temperature dependence of the critical field $H_{c1J}(T)$ for the YBCO junction. It linearly decreases with increasing T, but, remarkably, does not vanish at $T \to T_c$, as would be expected for conventional local Josephson junctions. As follows from Table I, the $H_{c1J}(T)$ depends on $I_c(T)$ and $\lambda(T)$, but the functional dependence is different for the local and the nonlocal cases. Figure 2(d) shows the T dependence of the critical current for the YBCO junction. It was obtained for the central maximum at zero field I_{c0} and the third sidelobe maximum I_{c3} (scaled by a factor 4).

Using the measured $H_{c1J}(T)$, $I_c(T)$, and the expressions for H_{c1J} from Table I, we calculate the $\lambda(T)$ dependence. Figures 2(e) and 2(f) represent the obtained $\lambda(T)$ and $\lambda^{-2}(T)$ for the overlap (local) [24] and planar (nonlocal) cases. It is seen that at low T there is no qualitative difference between the two models, which is probably the reason why a clear distinction could not be made from previous similar studies [3,9]. However, such a distinction becomes apparent from our data at elevated temperatures. From Figs. 2(e) and 2(f) it is seen that at $T > 70$ K the local theory provides totaly erroneous results with vanishing $\lambda(T)$ at $T \to T_c$. To the contrary, the nonlocal

theory provides both a quantitatively correct absolute value of $\lambda(0) \sim 0.2\ \mu$m at low T and a qualitatively correct T dependence at $T \to T_c$ with diverging $\lambda(T \to T_c)$ and linearly vanishing $\lambda^{-2}(T) \propto T_c - T$ [25,26]. The dotted horizontal line in Fig. 2(e) demonstrates that the divergence between local and nonlocal models occurs when $\lambda(T)$ becomes larger than the electrode thickness $d = 300$ nm. This indicates that a temperature-driven crossover from local to nonlocal electrodynamics takes place at $d \simeq \lambda(T)$.

Now we can understand why H_{c1J} does not vanish at $T \to T_c$ in our planar junctions. As seen from Table I, in the nonlocal model $H_{c1J}(T) \propto I_c(T)\lambda^2(T)$. From Figs. 2(d) and 2(f) it is seen that $I_c(T) \propto \lambda^{-2}(T) \propto T_c - T$ close to T_c. Therefore, H_{c1J} is determined by the ratio of two similar vanishing functions and remains finite at T_c. This is an intrinsic property and a consequence of nonlocal electrodynamics in planar thin-film Josephson junctions.

Our data indicate that the nonlocality strongly modifies properties of thin-film planar junctions, compared to that of conventional overlap junctions with local electrodynamics. The nonlocal effects can be large and crucial in a variety of experimental situations. Apart from the well-known quantitative difference, caused by flux focusing, here we demonstrate a dramatic qualitative difference in temperature dependencies of almost all junction characteristics. Figures 2(e) and 2(f) show that only by taking into account the nonlocality is it possible to correctly extract absolute values of the London penetration depth out of $I_c(H)$ data. The nonlocality significantly affects interaction between Josephson and Abrikosov (or Pearl) vortices and current-voltage characteristics in the flux-flow state [27]. It may also be useful for Josephson oscillators. Josephson emission is usually hampered by a large impedance mismatch between the junction and the outer space. The efficient emission requires electrode thicknesses larger than the radiation wavelength in vacuum [28]. For a THz frequency, this is 300 μm. It is practically impossible to make overlap junctions with so thick electrodes. But for planar junctions the thickness is replaced by the length, which is only limited by the size of the substrate. Thus, the long-range nonlocal stray fields in planar junctions may be more easily coupled to the vacuum field and provide better impedance matching with vacuum. The temperature range in which the nonlocality is crucial is determined by the inequality $d < \lambda(T)$. A typical value of $\lambda(T = 0)$ is 200 nm. Therefore, for thin-film junctions the temperature range is not limited to the vicinity of T_c. For example, our Nb junctions with $d = 70$ nm remain nonlocal in the full temperature range $0 < T < T_c$.

To conclude, we have studied the temperature dependence of the critical current modulation for low-T_c and high-T_c thin-film planar Josephson junctions. We observed a temperature-driven crossover from local to nonlocal electrodynamics. It takes place when $\lambda(T)$ becomes larger than the electrode thickness d. At elevated temperatures both

junctions exhibited a similar unusual behavior, which is in drastic discrepancy with that for conventional overlap-type junctions, described by the local sine-Gordon equation: (i) The flux-quantization field ΔH of $I_c(H)$ modulation was T independent, did not vanish at T_c, and was determined not by the London penetration depth λ but solely by the junction geometry w; (ii) the critical field for penetration of Josephson vortices H_{c1J} remained finite at the critical temperature T_c. These observations provided clear evidence for nonlocal electrodynamics in thin-film planar Josephson junctions in good agreement with theoretical predictions [4–7]. Our results indicate that the nonlocality indeed deeply affects properties of planar junctions.

[1] A. Barone and G. Paterno, *Physics and Applications of the Josephson Effect* (Wiley-Interscience, New York, 1982).

[2] Y. M. Ivanchenko and T. K. Soboleva, Phys. Lett. A **147**, 65 (1990).

[3] R. G. Humphreys and J. A. Edwards, Physica (Amsterdam) **210**, 42 (1993).

[4] R. G. Mints, J. Low Temp. Phys. **106**, 183 (1997).

[5] V. G. Kogan, V. V. Dobrovitski, J. R. Clem, Y. Mawatari, and R. G. Mints, Phys. Rev. B **63**, 144501 (2001).

[6] M. Moshe, V. G. Kogan, and R. G. Mints, Phys. Rev. B **78**, 020510(R) (2008).

[7] J. R. Clem, Phys. Rev. B **81**, 144515 (2010).

[8] P. A. Rosenthal, M. R. Beasley, K. Char, M. S. Colclough, and G. Zaharchuk, Appl. Phys. Lett. **59**, 3482 (1991).

[9] B. Mayer, S. Schuster, A. Beck, L. Alff, and R. Gross, Appl. Phys. Lett. **62**, 783 (1993).

[10] D. Winkler, Y. M. Zhang, P. A. Nilsson, E. A. Stepantsov, and T. Claeson, Phys. Rev. Lett. **72**, 1260 (1994).

[11] H. Hilgenkamp and J. Mannhart, Rev. Mod. Phys. **74**, 485 (2002).

[12] F. Tafuri and J. R. Kirtley, Rep. Prog. Phys. **68**, 2573 (2005).

[13] T. Akazaki, H. Takayanagi, J. Nitta, and T. Enoki, Appl. Phys. Lett. **68**, 418 (1996).

[14] V. M. Krasnov, T. Golod, T. Bauch, and P. Delsing, Phys. Rev. B **76**, 224517 (2007); V. M. Krasnov, O. Eriksson, S. Intiso, P. Delsing, V. A. Oboznov, A. S. Prokofiev, and V. V. Ryazanov, Physica (Amsterdam) **418**, 16 (2005).

[15] R. S. Keizer, S. T. B. Goennenwein, T. M. Klapwijk, G. Miao, G. Xiao, and A. Gupta, Nature (London) **439**, 825 (2006).

[16] T. Golod, A. Rydh, and V. M. Krasnov, Phys. Rev. Lett. **104**, 227003 (2010).

[17] R. W. Moseley, W. E. Booij, E. J. Tarte, and M. G. Blamire, Appl. Phys. Lett. **75**, 262 (1999).

[18] T. E. Golikova, F. Hübler, D. Beckmann, N. V. Klenov, S. V. Bakurskiy, M. Yu. Kupriyanov, I. E. Batov, and V. V. Ryazanov, JETP Lett. **96**, 668 (2013).

[19] D. Jeong, J. H. Choi, G. H. Lee, S. Jo, Y. J. Doh, and H. J. Lee Phys. Rev. B **83**, 094503 (2011).

[20] Ceraco ceramic coating GmbH, http://www.ceraco.de.

[21] A. M. Klushin, C. Weber, M. Darula, R. Semerad, W. Prusseit, H. Kohlstedt, and A. I. Braginski, Supercond. Sci. Technol. **11**, 609 (1998).

[22] A. M. Klushin, W. Prusseit, E. Sodtke, S. I. Borovitskii, L. Amatuni, and H. Kohlstedt, Appl. Phys. Lett. **69**, 1634 (1996).

[23] V. M. Krasnov, V. A. Oboznov, and N. F. Pedersen, Phys. Rev. B **55**, 14486 (1997).

[24] In the field perpendicular to films, the expression for H_{c1J} for overlap junctions should be corrected by the corresponding demagnetization factor, $H_{\text{eff}} = H/(1 - D)$.

We have chosen $D = 0.91$ to obtain the correct absolute value of λ at low T. This value of D is reasonable for our thin-film junctions.

[25] P. Zimmermann, H. Keller, S. L. Lee, I. M. Savić, M. Warden, D. Zech, R. Cubitt, E. M. Forgan, E. Kaldis, J. Karpinski, and C. Krüger, Phys. Rev. B **52**, 541 (1995).

[26] R. Prozorov and R. W. Giannetta, Supercond. Sci. Technol. **19**, R41 (2006).

[27] A. Gurevich, M. S. Rzchowski, G. Daniels, S. Patnaik, B. M. Hinaus, F. Carillo, F. Tafuri, and D. C. Larbalestier, Phys. Rev. Lett. **88**, 097001 (2002).

[28] L. N. Bulaevskii and A. E. Koshelev, Phys. Rev. Lett. **99**, 057002 (2007).